3rd International Conference on the Durability of Concrete Structures
17-19 September 2012
Queen's University Belfast
Paper Number SLM14

Investigation into the diffusivity of concrete using a three-dimensional multi-phase model

S. Deghanpoor Abyaneh, H.S. Wong, and N.R. Buenfeld
Concrete Durability Group, Department of Civil and Environmental Engineering, Imperial College London

ABSTRACT

This paper presents a numerical investigation into the diffusivity of cement-based materials. Concrete is treated as a three-phase interactive composite consisting of aggregate particles, bulk cement paste and aggregate-paste interface, i.e. the 'interfacial transition zone' (ITZ). The model is set up in two stages. First, a three-dimensional representative volume element of the concrete microstructure is generated. Then, a finite difference method is used to simulate molecular diffusion through the microstructure. The transport properties of the conductive phases (bulk cement paste and ITZ) are determined based on the water/cement ratio, degree of hydration and conservation of porosity in the microstructure. The model is validated against analytical relationships for ideal cases and against available experimental data. The model is then applied to perform a sensitivity analysis to evaluate the effects of aggregate content, water/cement ratio and degree of hydration on diffusivity.

1. INTRODUCTION

Diffusion is one of the most important transport processes influencing the durability of cement-based materials. Therefore, the ability to estimate the diffusivity of concrete based on mixture proportions and microstructure is attractive, as it would allow the development of service life prediction models and durability-based design codes.

Lab based transport testing has been carried out for many years to gain a better understanding of different variables influencing the transport properties of cement-based materials. Since the microstructure of concrete is highly complex and its transport properties are influenced by many interacting parameters, many experiments should be carried out in order to identify the effect of different variables. However, it is often difficult to isolate the effects of specific variables because other influencing parameters inevitably vary. While some of these effects can be reduced or avoided entirely, others are difficult if not impossible to control, and so must be accounted for when analysing results. Moreover, experiments are time-consuming and expensive.

The tremendous increase in computational capabilities has strongly favoured the development of numerical simulations based on rather precise description of the microstructure. However, it is still not possible to simultaneously model concrete in a single model because of the wide range of feature sizes, from the nanometre-sized pores to millimetre-sized aggregates, and memory limitations. Therefore, it is necessary to combine several models at different length scales. Multi-scale modelling techniques offer a promising solution to this restriction. In this approach, properties computed at one scale, micrometers for instance, are input into a model that is constructed at a higher scale, such as millimetres.

Bentz et al. (1998) used random walk simulations to study the diffusivity of concrete. Concrete is assumed as a composite material consisting of aggregates, ITZ and bulk cement paste, and all three phases are treated as uniform continuum materials. Kamali-Bernard et al. (2009) computed the diffusivity of mortars from a digitized mesostructure by applying Fick's law. However, the mortar is assumed as a 'simple' composite, in which the transport properties of the conductive phases (bulk cement paste and ITZ) are constants obtained by fitting experimental results. Zheng et al. (2009) proposed a three-phase composite sphere model to predict the steady-state chloride diffusivity of concrete. However, the simplified microstructure may not be sufficient to capture the effects of ITZ percolation and tortuosity of multi-sized aggregates.

This paper presents a numerical investigation into the diffusivity of mortars and concretes. The developed model is regarded as 'interactive' because the transport properties of the ITZ and bulk paste are estimated from their porosities, which depend on the ITZ characteristics (width, porosity gradient), water/cement ratio and degree of hydration. Thus, the total porosity (ITZ + bulk paste) is 'conserved' and is equal to the porosity of a cement paste of the same w/c ratio and hydration degree. Furthermore, a realistic aggregate size distribution is used as an input to the model. The

main purpose of this work is to determine the main parameters influencing diffusivity. The model was validated against available theoretical and experimental results and was then applied to evaluate the effects of aggregate content, water/cement ratio and degree of hydration on diffusivity.

2. METHODOLOGY

In order to model transport phenomena in any material, e.g. cement-based materials, one needs a structure as an input coupled with a transport algorithm. So, our method operates in two main steps. First, a three-dimensional voxelised mesostructure of concrete is generated. Concrete is treated as a three-phase composite material, consisting of aggregates, bulk cement paste and ITZ. The model can also include other phases such as air voids or cracks. Second, in order to simulate the diffusion process, a finite difference scheme is applied to the mesostructure. For simplicity, we will only consider the case of diffusion under saturated and steady-state conditions in this study, but we note that this is not a limitation of the method. In this study, saturated means that the total porosity is available for transport.

This approach has several advantages. Firstly, a rather precise description of the microstructure is used as an input. Secondly, as the input structure is voxelized, other transport properties such as pressure-induced flow and capillary absorption can also be simulated using the appropriate lattice methods. Thirdly, the model serves as a platform for using real images of microstructure as input. Finally, the finite difference technique requires much less memory compared to finite element methods. Thus investigation of higher discretization levels which can lead to better accuracy is possible.

3. DESCRIPTION OF THE MODEL

3.1. GENERATION OF NUMERICAL SAMPLE

The number of aggregate particles in the mesostructure is first determined from grading curves. Each class of aggregates is replaced by identical digitized spheres of the required volume fraction. The aggregates are placed randomly (larger aggregates first) and they are not allowed to overlap. Periodic boundary conditions are applied on all sides of the computational cube to minimize size effects. Then the aggregates are coated with voxels representing the 'interfacial transition zone' (ITZ). A large number of voxels is probably required to realistically represent the ITZ, but this comes at the cost of higher memory and computational time requirements. This effect will be examined in the following sections and the necessary number of ITZ voxels will be determined. Figure 1 shows an example of a typical mesostructure for a mortar.

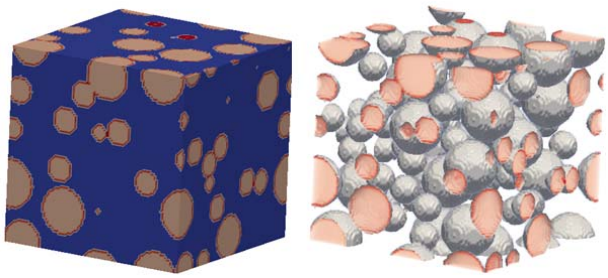

Figure 1. Typical mesostructure of mortar with spherical aggregates (5mm cube).

Representing aggregates as spherical particles is probably a gross simplification. However, reported results on the effect of aggregate shape on mass transport properties of cement-based materials appear to be ambiguous and are mostly conducted in two dimensions (Li et al., 2012; Zheng et al., 2012). The effect of this simplifying assumption can be readily examined using the proposed approach.

3.2 DIFFUSIVITY OF DIFFERENT PHASES

Once the mesostructure is obtained, numerical techniques such as finite element and finite difference can be employed to characterise the bulk transport property. Prior to application of these numerical techniques, the transport property of each component in the mesostructure must be determined. In this study, we will only need to consider the transport properties of the aggregates, ITZ and bulk cement paste.

Aggregates are assumed impermeable and they are assigned "zero" as their transport property. However, the presence of aggregates perturbs the surrounding cement paste. This perturbed zone, known as the 'interfacial transition zone', shows different characteristics compared to the 'bulk' cement paste. Its origin lies in the inefficient packing of cement grains against the much larger aggregate, which leads to a higher effective w/c ratio and porosity at the ITZ compared to the 'bulk' paste. Because of the packing effect, more water is incorporated in the ITZ and the effective water to cement ratio of the "bulk" paste is reduced (Scrivener et al., 2004). During hydration, the porosity decreases throughout the cement paste, but remains higher in the ITZ.

Figure 2 shows the measured average porosity gradient near the aggregate surface for an OPC concrete with a water/cement ratio of 0.4 after 28 days curing, obtained from the work of Crumbie (1994). The porosity in ITZ, $\phi(x)$ can be represented by an exponential function of distance from aggregate x:

$$\phi(x) = \phi_{bcp} + 0.2\exp(-0.07x) \quad (1)$$

where ϕ_{bcp} is the porosity of bulk cement paste. It is assumed that the shape of the curve is independent of w/c ratio and degree of hydration, and that the porosity gradient only shifts vertically when the w/c ratio or degree of hydration is varied (Bentz and Garboczi, 1991; Crumbie, 1994; Scrivener et al., 2004; Scrivener and Nemati, 1996). However, it should be noted that although the average ITZ porosity shows strong well-defined gradients, the local porosity, width and gradient are highly variable. The porosity gradient could also be influenced by the amount of calcium hydroxide precipitated on aggregate surfaces (Wong and Buenfeld, 2006). For the sake of simplicity, we will use the exponential function shown in Eq. 1 to represent the porosity gradient around every aggregate particle.

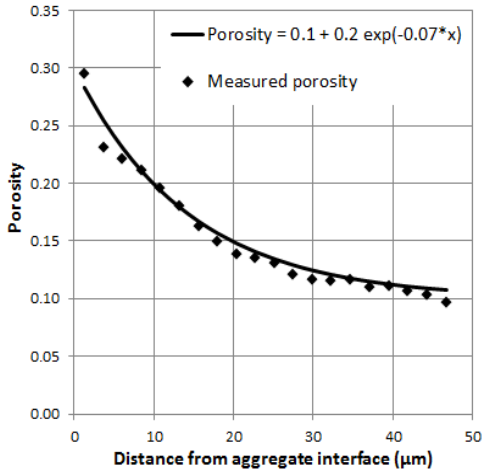

Figure 2. Average porosity in the ITZ as a function of the distance from the aggregate surface for an OPC concrete with w/c = 0.4 after 28 days (Crumbie, 1994)

The diffusivity of the bulk cement paste and ITZ are determined as follows:

(1) The total capillary porosity of cement paste is estimated from the w/c ratio and degree of hydration (α) based on the work of Powers and Brownyard (1947) as modified by Young and Hansen (1987):

$$\Phi_{hcp} = 1 - \frac{1+1.31\alpha}{1+3.2\frac{w}{c}} \quad (2)$$

(2) The ratio of porosity of ITZ over porosity of bulk cement paste is estimated using Eq. 1 for a particular ITZ gradient.

(3) The porosity of ITZ and bulk cement paste is then obtained from the equation of conservation of porosity:

$$V_{bcp}\Phi_{bcp} + V_{ITZ}\Phi_{ITZ} = (V_{bcp} + V_{ITZ})\Phi_{hcp} \quad (3)$$

where ϕ_{bcp} and ϕ_{ITZ} are the porosities of the bulk cement paste and ITZ respectively. V_{bcp} and V_{ITZ} are the volume fractions of the bulk cement paste and ITZ, which are obtained from the mesostructure.

(4) Once the ITZ porosity is known, the relative diffusivity, D/D_0, as a function of distance from the aggregate surface, x, can be estimated using the following equation (Garboczi and Bentz, 1992):

$$\frac{D}{D_0}(x) = 0.001 + 0.07\Phi(x)^2 + 1.8H(\Phi(x) - 0.18) \times (\Phi(x) - 0.18)^2 \quad (4)$$

where relative diffusivity is the ratio of diffusivity in the material of interest D to the free diffusivity, D_0, $\phi(x)$ is the capillary porosity at a distance x from an aggregate surface, and H is the Heaviside function having a value of 1 when $\phi > 0.18$ and a value of 0 otherwise. This equation comes from fitting the results of several cement pastes at different w/c ratios (0.4 to 0.6), and degrees of hydration (0.5 to 0.9). The constant term in this equation comes from the limiting value of diffusion through C-S-H gel pores, when the capillary porosity is zero, the H term represents diffusion through percolated capillary porosity, and the second term in the equation is a fitting term that connects the two limiting behaviors. Although Eq. 4 is not exact, it has been shown to give results accurate to at least a factor of two for absolute diffusivity, and better for relative diffusivity (Garboczi and Bentz, 1992).

(5) The diffusivity of bulk cement paste can also be obtained by Eq. 4 once the porosity of bulk cement paste is calculated.

(6) The ITZ can be divided into several layers where the diffusivity of each layer is obtained by averaging the local relative diffusivities in that layer.

Our approach captures the effect of porosity gradient in the ITZ, in contrast to random walk methods. However, it is computationally expensive since many voxels are required in order to realistically represent ITZ. So hereinafter, the diffusivities of voxels lying in the ITZ region are assumed to be the same. Other phases such as cracks and air voids can also be included in the mesostructure model if required. The transport characteristics of air voids can be assigned depending on whether the air voids act as conductors or insulators (Wong et al., 2011).

3.3 SIMULATION OF DIFFUSION PROCESS

Diffusion through porous media is usually described by Fick's laws. Fick's first law relates the flux to concentration gradient through a constant which is the diffusion coefficient:

$$J = D\nabla C \quad (5)$$

Coupling Fick's first law with mass conservation, Fick's second law is derived:

$$\frac{\partial c}{\partial t} = \nabla(D\nabla C) \quad (6)$$

When steady state is reached, the left hand side of the equation vanishes:

$$\nabla(D\nabla C) = 0 \quad (7)$$

Since the mesostructure is digitized into voxels, in order to get a finite difference form of Eq. 7, the partial derivatives of concentration should be expanded around the centers of the voxel of interest, voxel *i*, to obtain:

$$C_i = \frac{\sum_j D_{ij} C_j}{\sum_j D_{ij}} \quad (8)$$

where D_{ij} is the effective diffusion coefficient of the element relating the voxel *i* to voxel *j*. *j* represents the voxels neighboring voxel *i*. As the aggregates are assumed to be impermeable, Eq. 8 is written only for the nodes lying in the ITZ and bulk cement paste.

When two voxels share a face, see Fig. 3, and are of the same phase, the diffusivity of the element connecting them is the diffusivity of that particular phase. If the two face-sharing voxels are of different phases, the diffusivity of the element connecting them is approximated as a series combination of one half the diffusivity of each voxel. When two voxels share a vertex or an edge, no connection is assumed between them in the finite difference scheme. So in our model, flow is only possible through the nearest neighbor connections.

If one assumes ITZ as a single uniform layer, then three cases may occur for the elements relating voxels *i* and *j*. First, if *i* and *j* both represent bulk cement paste, diffusivity of bulk cement paste will be assigned to the element *ij*. Second, diffusivity of ITZ will be assigned to the element relating two voxels of ITZ. Third, if *i* and *j* represent ITZ and bulk cement paste or the inverse, the diffusivity of the element can be approximated using a series combination of one half of ITZ and one half of bulk cement paste:

$$\frac{2}{D_{ITZ-bulk\ cement\ paste}} = \frac{1}{D_{ITZ}} + \frac{1}{D_{bulk\ cement\ paste}} \quad (9)$$

If one assumes the ITZ as a series of layers each having its own porosity and transport property, then many more cases may occur for the elements relating voxels *i* and *j*. We would have one case for the bulk cement paste and others for the ITZ layers depending on the distance from the surface of aggregate. Similar rules should apply when determining the connectivity and diffusivity of the element relating voxels i and j as described earlier.

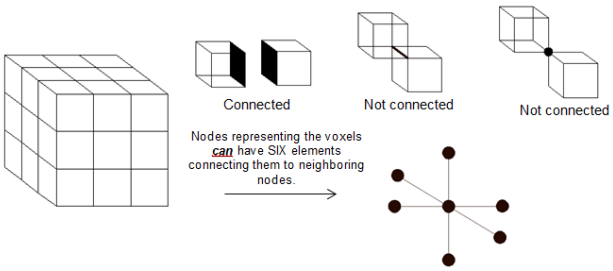

Figure 3. Schematic diagram showing the connectivity of elements in the voxelized mesostructure.

A constant boundary condition is applied for all the nodes on the inlet and outlet surfaces. For the outlet surface, zero concentration is imposed on all nodes. For the inlet surface, a constant concentration is applied. Eq. 8 will lead to a set of algebraic simultaneous equation which can be solved by an iterative algorithm such as the Gauss-Seidel method. Once the concentration in all the nodes is obtained, the diffusion coefficient (diffusivity) of the media can be calculated as

$$D_e = \frac{QL}{A\Delta C} \quad (10)$$

where *Q* is the summation of the flow in all elements which intersect the outlet surface, *A* is the cross section area and *L* is the length over which the concentration gradient is imposed.

4. REPRESENTATIVE ELEMENTARY VOLUME

Since the model uses a three-dimensional voxelized microstructure as input and applies finite difference to simulate diffusivity, it is therefore potentially subjected to effects of digital resolution, finite size error and statistical fluctuation. Obviously, one can decrease these effects respectively by increasing the resolution, sample size and averaging over a number of realisations. However, this increases the computational expense. Thus, it is important to determine the minimum requirements to obtain satisfactory results.

4.1 SIZE EFFECT AND STATISTICAL FLUCTUATION

Statistical fluctuation errors are due to the random nature of the system, while finite size effect errors arise because the physical size of the model is usually small to speed up computation. In order to evaluate the effects of finite size and statistical fluctuation on the results, we simulated the diffusivity for different numerical sample sizes at several realisations. Figures 4 and 5 show the results.

The created mesostucture has a random structure because random numbers are used to determine where the aggregate particles are placed. Thus, there will be some differences between different realizations, as shown in Figures 4 and 5. It can also be observed that the precision of replicate simulations improves with increase in sample size.

However, the actual variability is very small (to the third decimal point). It should also be noted that the unit cells have periodic boundary conditions, which greatly reduce any surface effects. The results show that a model consisting of unit cells that are at least 2.5 times the maximum aggregate size is sufficiently large to be representative. In all the simulations hereinafter, this criterion will be satisfied.

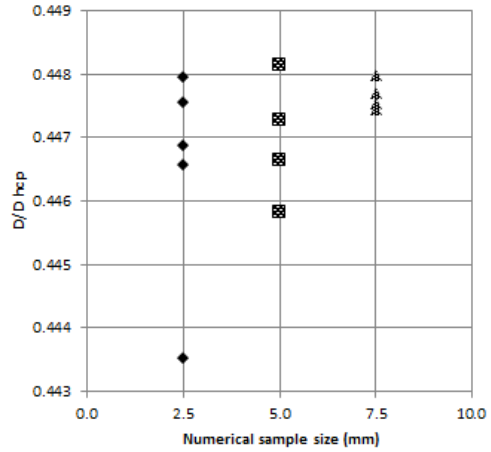

Figure 4. Simulated diffusivity ratio D/D_{hcp} (No ITZ, V_a = 40%, aggregate gradation = 0.15 – 1 mm, Fuller)

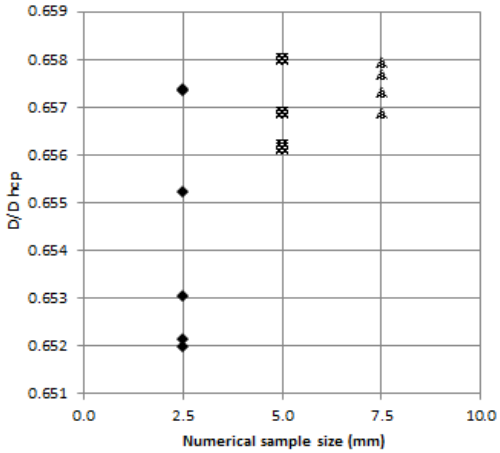

Figure 5. Simulated diffusivity ratio D/D_{hcp} (ITZ width = 50 μm, w/c = 0.5, degree of hydration = 80%, V_a = 40%, aggregate gradation = 0.15 – 1 mm, Fuller)

4.2 EFFECT OF RESOLUTION

This model, similar to any other model that uses digitized microstructure as an input, idealises continuum shapes with a certain degree of resolution. The higher the resolution, the better the accuracy. However, the available computational resource imposes a practical limit on the resolution used for each simulation. Prior to using the model for investigation and prediction of transport properties, the effect of resolution should be examined.

4.2.1 NECESSARY RESOLUTION TO CAPTURE THE EFFECT OF AGGREGATES

The presence of impermeable aggregates in the cement paste matrix has two opposite effects on the transport properties. First, it reduces the transport property by decreasing the volume of cement paste (dilution) and increasing the conduction paths by redirecting conduction around aggregates (tortuosity). On the other hand, the formation of porous ITZ and its percolation may drastically increase transport properties.

In order for the model to capture the effects of dilution and tortuosity due to the presence of aggregates, the shape of aggregates should be represented as realistically as possible. To determine the necessary resolution for capturing the dilution and tortuosity, we computed the diffusivity of a mortar which has 50% sand volume fraction and aggregate size ranging from 0.15 to 2 mm (Fuller gradation). Table 1 shows the computed diffusivities at five different resolutions carried out at a fixed sample size of 5mm cube. In the first case, the smallest aggregate is represented by a sphere with a radius of 2 voxels. Spheres of radius 3, 4, 5 and 6 voxels are used in the other cases. It should be recalled that the presence of ITZ is ignored at this stage since we want to examine only the effect of dilution and tortuosity. It was observed that the final three attempts (R=4, R=5, R=6) lead to a similar result.

Table 1. Calculated diffusivity ratio of mortar with 50% sand volume fraction (R=2, R=3, R=4, R=5 and R=6 correspond to the average results obtained for five different resolutions)

R=2	R=3	R=4	R=5	R=6	*Analytical result*
0.31	0.33	0.35	0.35	0.35	0.35

It is also interesting to compare the simulated values with available analytical results. According to the Bruggeman-Hanai law, the effective conductivity (diffusivity) of a media containing spherical non-conductive particles which are embedded in an otherwise homogeneous matrix can be calculated using Eq. 11.

$$\frac{D}{D'} = (1 - V_a)^{3/2} \qquad (11)$$

where V_a is the volume fraction of spherical particles, D' is the conductivity (diffusivity) of homogeneous matrix and D is the effective conductivity (diffusivity). This formula is based on the assumption that the conductivity of the matrix is constant as non-conductive particles are added, therefore it captures the effects of dilution and tortuosity, and not the ITZ (Bruggeman, 1935; McLachlan et al., 1990). As shown in Table 1, an excellent agreement was observed between the simulated results (R=4, R=5, R=6) with this formula. Therefore, it can be concluded that the smallest spherical aggregate used in this model should at least have a radius of 4 voxels to capture the effects of dilution and tortuosity. Using this resolution, we calculated the diffusivity of mortars containing varying aggregate volume fraction (no

ITZ). Figure 6 shows the simulated values plotted against aggregate volume fraction. Once again, a good agreement with the Bruggeman-Hanai law is observed.

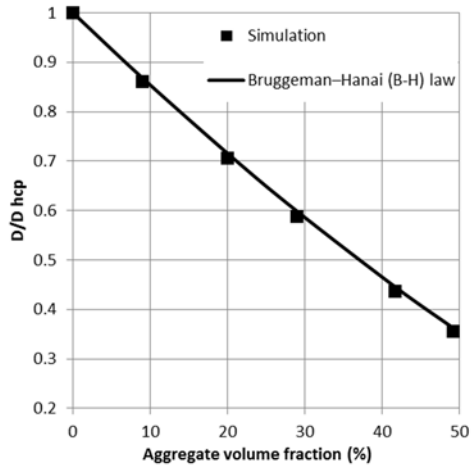

Figure 6. Comparison between the simulated D/D_{hcp} and analytical results from the Bruggeman-Hanai equation.

4.2.2 NECESSARY RESOLUTION TO CAPTURE THE EFFECT OF ITZ

Considering that the ITZ thickness is typically in the order of 25 to 50 μm, the voxel size should be at most equal to this value so that the effect of ITZ can be modelled. Increasing the number of voxels (by decreasing the voxel size) representing the ITZ could lead to better accuracy. Figure 7 shows the effect of number of ITZ voxels on the simulated diffusivity of a mortar. As expected, increasing the number of ITZ voxels increases the simulated transport property because the connectivity of the ITZ is better represented when smaller voxels are used. However, this comes at a cost of higher computational requirements. Our results show that using at least a two-voxel thick ITZ seems to be good compromise. This means that a 25 μm voxel would be necessary to represent a 50 μm thick ITZ.

Hereinafter, the size of voxel used to digitise our mesostructure will be selected based on the criteria that the radius of the smallest aggregate particle is at least 4 voxels and that the ITZ is at least 2 voxels thick. On a single 64-bit PC (3.4 GHz processor), the simulation time for the results shown here, is between 5 minutes and three hours depending on the size and volume fraction of aggregates. The highest memory consumption is less than 2 GB.

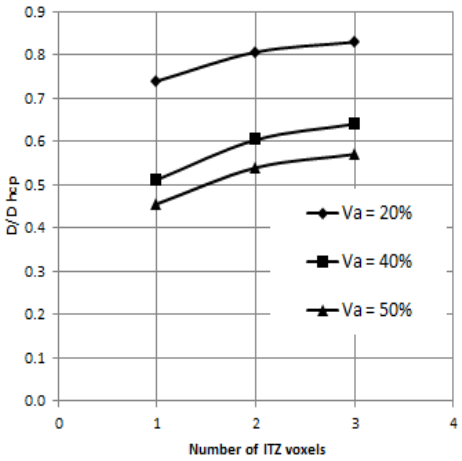

Figure 7. Effect of the number of voxels representing ITZ width on the calculated diffusivity ratio D/D_{hcp} for various aggregate volume fractions V_a (ITZ width = 50 μm, w/c = 0.5, degree of hydration = 80%, aggregate gradation = 0.15 – 2 mm, Fuller).

5. RESULTS

5.1 COMPARISON WITH EXPERIMENTAL DATA

In this section, we compare the simulated diffusivities from the model with available experimental results. To carry out this comparison, the degree of hydration of the sample is required. Unfortunately, in most experimental studies, while the age of the sample at the time of testing is given, no information about the degree of hydration is provided.

The first set of experimental data to which the results of this model will be compared is from Wong et al. (2009). They measured the oxygen diffusivity of mortars containing 0-55% volume fraction of sand. The sand used was < 5 mm and complied with the BS 882 medium grading. Oxygen diffusivity was determined by exposing the opposite faces of the sample to a stream of oxygen and nitrogen at equal pressure. The oxygen concentration at steady state in the outflow stream was measured using a zirconia analyser to calculate diffusivity. The degree of hydration was also determined from the non-evaporable water content measured by loss-on-ignition of the cement paste. Figure 8 compares the numerical simulations with experimental results for mortars at w/c ratio 0.3 that were sealed cured for 3 days prior to testing. Note that the actual aggregate size distribution from Wong et al. (2009) was used as input to the model. The measured degree of hydration for the 0.3 w/c ratio pastes cured for 3 days were 0.56. Generally, a good agreement is observed.

The second set of data from Delagrave et al. (Delagrave et al., 1997), consists of mortars made at 0.45 w/c ratio containing 0.15–0.6 mm crushed siliceous sand at 0%, 30% and 50% volume fractions. 15 mm thick samples were cured in saturated lime solution for 3 months and then

vacuum saturated in deionised water and tested using a migration cell technique similar to the one described by Buenfeld and El-Belbol (Buenfeld and El-Belbol, 1991). The upstream compartment of the migration cell was filled with a 0.5 M NaCl in 0.3 M NaOH solution, and a 10 V potential was applied across the cell. The chloride concentration in the downstream compartment was monitored for 3 weeks and the migration coefficient was obtained from the steady-state regime according to the Nernst–Plank equation.

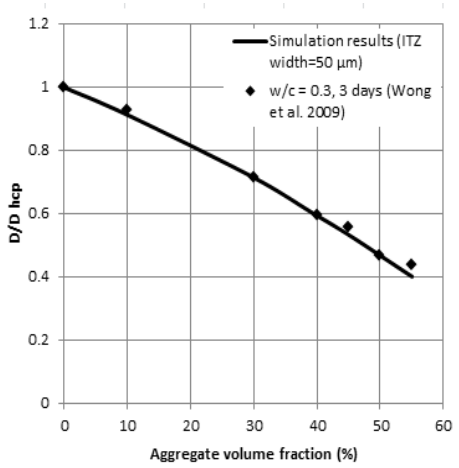

Figure 8. Comparison between numerical simulations with experimental results of Wong et al. (Wong et al., 2009).

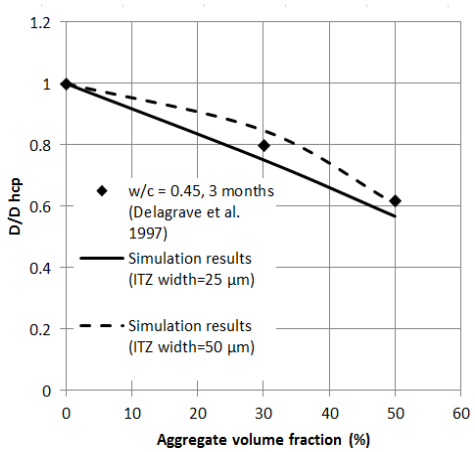

Figure 9. Comparison between the numerical simulations and experimental results of Delagrave et al. (1997).

In order to compare the experimental results with the numerical simulation, an estimate of the degree of hydration of the mortars tested by Delagrave et al. (1997) is required. A value of 0.84 will be assumed, consistent with the value used by Bentz et al. (2000) and Kamali-Bernard et al. (2009). Figure 9 compares our numerical simulations with the experimental results, which are plotted against aggregate volume fraction. Note that the actual aggregate size distribution from the original reference was used as input to our model. The simulations were carried out at ITZ widths of 25µm and 50µm.

5.2 SENSITIVITY ANALYSIS

A sensitivity analysis was performed using the proposed model to examine the relative influence of water cement ratio, degree of hydration and aggregate volume fraction on diffusivity. Our results are in general agreement with the findings of Zheng et al. (2009).

5.2.1 WATER TO CEMENT RATIO

Figure 10 shows the effect of water to cement ratio on the simulated diffusivity of mortar. As expected, the diffusivity reduces substantially with the decrease in water to cement ratio. The diffusivity also reduces significantly with the increase in aggregate content. The diffusivity decreases despite the fact the ITZ is percolated at high aggregate volume fractions.

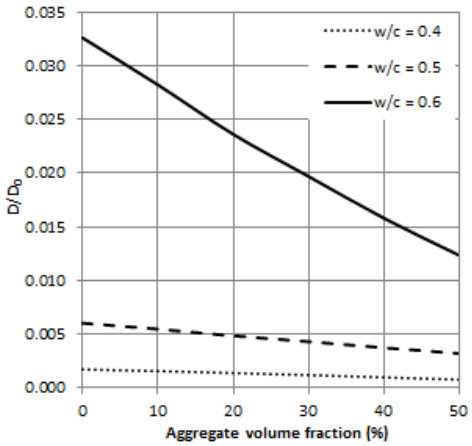

Figure 10. Effect of water to cement ratio on the simulated D/D_0 (ITZ width = 50 µm, degree of hydration = 80%, aggregate gradation = 0.15 – 2 mm, Fuller).

5.2.2 DEGREE OF HYDRATION

Fig. 11 shows the effect of degree of hydration on the simulated diffusivity of mortar. For samples with equal water to cement ratio and aggregate content, diffusivity decreases with the increase in degree of hydration (increase in curing age). The diffusivity also reduces significantly with the increase in aggregate content and no ITZ percolation threshold was observed.

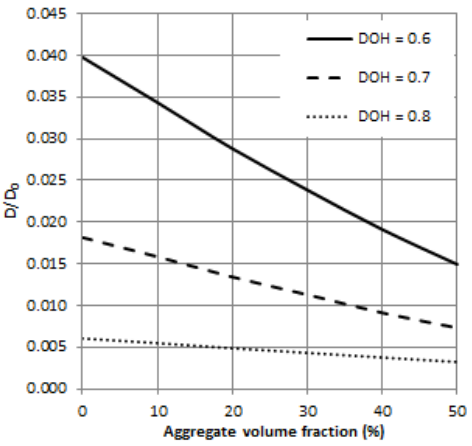

Figure 11. Effect of degree of hydration on the simulated D/D_0 (ITZ width = 50 µm, w/c = 0.5, aggregate gradation = 0.15 – 2 mm, Fuller).

6. CONCLUSIONS

This paper presented an investigation into the diffusivity of cement-based materials using a three-phase interactive composite model. Inputs to the model are the aggregate particle size distribution and volume fraction, w/c ratio, degree of hydration and ITZ porosity gradient. The required voxel resolution to capture the effects of dilution, tortuosity and ITZ were examined. The validity of the developed model was verified by comparing with two sets of experimental results. The model was then applied to examine the influence of several parameters on diffusivity. It was found that diffusivity decreases with increase in aggregate volume fraction and degree of hydration, but increases with increase in water to cement ratio. These parameters are significant because they control the total porosity of the composite. Our results are in general agreement with the findings of Zheng et al. (2009).

ACKNOWLEGMENTS

The research leading to these results has received funding from the European Union Seventh Framework Programme (FP7 / 2007-2013) under grant agreement 264448.

REFERENCES

Bentz, D.P., Garboczi, E.J., 1991. Simulation studies of the effects of mineral admixtures on the cement paste-aggregate interfacial zone. ACI Materials Journal, 88(5): 518-529.

Bentz, D.P., Garboczi, E.J., Lagergren, E.S., 1998. Multi-scale microstructural modeling of concrete diffusivity: Identification of significant variables. Cement Concrete and Aggregates, 20(1): 129-139.

Bruggeman, D.A.G., 1935. Berechnung verschiedener physikalischer Konstanten von heterogenen Substanzen. I. Dielektrizitätskonstanten und Leitfähigkeiten der Mischkörper aus isotropen Substanzen. Annalen der Physik, 416(7): 636-664.

Buenfeld, N.R., El-Belbol, S., 1991. Rapid estimation of chloride diffusion coefficient in concrete - comment. Magazine of Concrete Research, 43(155): 135-139.

Crumbie, A.K., 1994. Characterisation of the microstructure of concrete, Imperial College London.

Delagrave, A., Bigas, J.P., Ollivier, J.P., Marchand, J., Pigeon, M., 1997. Influence of the interfacial zone on the chloride diffusivity of mortars. Advanced Cement Based Materials, 5(3-4): 86-92.

Garboczi, E.J., Bentz, D.P., 1992. Computer simulation of the diffusivity of cement-based materials. Journal of Materials Science, 27(8): 2083-2092.

Kamali-Bernard, S., Bernard, F., Prince, W., 2009. Computer modelling of tritiated water diffusion test for cement based materials. Computational Materials Science, 45(2): 528-535.

Li, L.-Y., Xia, J., Lin, S.-S., 2012. A multi-phase model for predicting the effective diffusion coefficient of chlorides in concrete. Construction and Building Materials, 26(1): 295-301.

McLachlan, D.S., Blaszkiewicz, M., Newnham, R.E., 1990. Electrical resisivity of composites. Journal of the American Ceramic Society, 73(8): 2187-2203.

Powers, T.C., Brownyard, T.L., 1947. Studies of the physical properties of hardened cement paste. J. Am. Concr. Inst. , 43.

Scrivener, K.L., Crumbie, A.K., Laugesen, P., 2004. The interfacial transition zone (ITZ) between cement paste and aggregate in concrete. Interface Science, 12(4): 411-421.

Scrivener, K.L., Nemati, K.M., 1996. The percolation of pore space in the cement paste aggregate interfacial zone of concrete. Cement and Concrete Research, 26(1): 35-40.

Wong, H.S., Buenfeld, N.R., 2006. Euclidean Distance Mapping for computing microstructural gradients at interfaces in composite materials. Cement and Concrete Research, 36(6): 1091-1097.

Wong, H.S., Pappas, A.M., Zimmerman, R.W., Buenfeld, N.R., 2011. Effect of entrained air voids on the microstructure and mass transport properties of concrete. Cement and Concrete Research, 41(10): 1067-1077.

Wong, H.S., Zobel, M., Buenfeld, N.R., Zimmerman, R.W., 2009. Influence of the interfacial transition zone and microcracking on the diffusivity, permeability and sorptivity of cement-based materials after drying. Magazine of Concrete Research, 61(8): 571-589.

Young, J.F., Hansen, W., 1987. Volume Relationships for C-S-H Formation Based on Hydration Stoichiometries. Materials Research Society Symposium Proceedings, 85: 313–322.

Zheng, J.-J., Wong, H.S., Buenfeld, N.R., 2009. Assessing the influence of ITZ on the steady-state chloride diffusivity of concrete using a numerical model. Cement and Concrete Research, 39(9): 805-813.

Zheng, J.-J., Zhou, X.-Z., Wu, Y.-F., Jin, X.-Y., 2012. A numerical method for the chloride diffusivity in concrete with aggregate shape effect. Construction and Building Materials, 31(0): 151-156.